

Phase Contrast Imaging with High Resolution Cone Beam X-ray Computed Tomography

Johann KASTNER, Bernhard PLANK, Dietmar SALABERGER
Upper Austrian University of Applied Sciences, Wels Campus
Stelzhamerstrasse 23, A-4600 Wels

Abstract. X-ray computed tomography (XCT) with cone beam geometry has become a very important method for non-destructive 3D-characterisation and evaluation of materials. Compact XCT systems can reach resolutions down to 1 μm and even below. However, the polychromatic nature of the source, limited photon flux and the consequent long measurement times as well as all kinds of measurement artifacts lead to limitations concerning the achievable XCT-data quality and resolution. Another aspect of high resolution XCT is the possibility of phase contrast imaging even for polychromatic sources, which can lead to significant improvements over conventional attenuation-based X-ray computed tomography. Phase contrast can increase the visibility of small structures by edge enhancement. This can be especially advantageous for small structures, soft materials and material systems with small differences in attenuation.

First, we report on the stabilisation of the XCT-device by using tube cooling. The heat generated at the target and at the deflection coils causes expansion of the whole tube and therefore to movement of the focal spot. The effect of these movements was investigated by measuring the position of copper wires that were mounted at different positions. The proper use of the cooling results in a significant improvement in image quality and resolution. This improvement is demonstrated by XCT-measurements with a voxel size of 500 - 700 nm for a polypropylene-sample filled with talcum, a wood sample, polyurethane foam filled with cellulose particles and the Al-alloy AlMg5Si7.

Secondly, we report on the possibilities of phase contrast imaging using a cone beam XCT device with a polychromatic nano-focus tube source. The influence of various parameters like voxel size/resolution, energy of the X-ray source, X-ray-source-detector distance, and object-detector distance on the phase contrast amplitude is presented. The correspondence of the experimental results to theoretical considerations is discussed. The advantages and limitations of phase contrast imaging for various material systems like carbon-fibre reinforced polymers and the Al-alloy AlMg5Si7 are presented and discussed.

1. Introduction and Motivation

X-ray computed tomography (XCT) with cone beam geometry is a non-destructive imaging technique to generate volumetric representations from a series of 2D X-ray projection images usually based on X-ray absorption. The main advantage of XCT is comprehensive characterisation of the internal and external structures of a specimen as well characterisation of various phases present in the material [1, 2]. When X-ray attenuation



coefficients at the interface between two different materials are too close, conventional absorption-based methods can fail to show a significant difference in the resulting grey-values. In such cases phase-imaging methods can increase the contrast significantly. This is well known for synchrotron radiography and synchrotron tomography, where highly coherent X-ray beams are used [3, 4]. Wilkins et al. found in 1996 [5] that a polychromatic source with high spatial coherence such as an ideal point source can reveal a significant phase contrast. There are several publications about the application of tube-based phase contrast radiography for medical applications [3, 5, 6] and also some publications about phase contrast radiography for non-destructive testing of materials [7, 8].

The main goal of this publication is the utilisation of polychromatic cone-beam XCT for the non-destructive evaluation of materials by absorption and phase contrast tomography. An optimised high resolution XCT-system with a tube cooling system and a voxel size below 1 μm is used to scan various materials and to investigate the advantages and limitations of high resolution XCT.

2. Experimental

Various materials like polypropylene filled with talcum, pinewood, polyurethane foam filled with cellulose particles, the light metal alloy AlMg5Si7 and a carbonfibre reinforced polymer (CFRP) were investigated by high resolution X-ray computed tomography. The tomograms were scanned using a “nanotom 180NF XCT” desktop device developed and manufactured by GE Sensing & Inspection Technologies phoenix|x-ray equipped with a 180 keV high power nano-focus tube with transmitting target and a 2300x2300 pixel Hamamatsu detector [9]. A target made of molybdenum was used at a voltage between 50 and 60 kV. The X-ray tube of the “nanotom” is equipped with an external liquid cooling system to ensure stable measurement conditions and to minimise thermal influences during scans of longer duration. Table 1 gives an overview of the most important measurement parameters.

Table 1. XCT measurement parameters: voxel size (VS), tube voltage (U), tube current (I), integration time at the detector (t_{int}), number of projections (n), measurement time (t_{mes}), and the distance between the object and the detector ODD.

Sample	VS [μm]	U [kV]	I [μA]	t_{int} [ms]	n	t_{mes} [min]	ODD (mm)
Polypropylene filled with talcum (measured without tube cooling)	0.7	50	300	1500	2000	349	197.2
Polypropylene filled with talcum (with tube)	0.7	50	450	1500	2000	414	197.2
Pinewood	1.5	60	430	1750	1600	428	194
Pinewood	0.5	60	430	1750	1600	428	198
Polyurethane foam filled with cellulose	0.5	50	450	1250	1700	294	198
AlMg5Si7	0.5	60	410	2000	1700	600	497.5
Carbon-fibre reinforced polymer	2.75	60	240	2000	900	180	189
Carbon-fibre reinforced polymer	2.75	60	240	4000	900	360	283.5
Carbon-fibre reinforced polymer	2.75	60	230	2250	1800	405	486

3. Results and Discussion

3.1 Investigations on stability and tube cooling

One goal of this investigation was the optimisation of XCT-data quality by using tube cooling for the XCT device. The heat generated at the target and at the deflection coils leads to expansion of the whole tube and therefore to movement of the focal spot and the whole system. The effects of these movements were investigated by measuring the position of copper wires that were mounted on the tube and also fixed to the turntable. The use of the cooling results in a significant decrease in movement of the tube. As seen in Fig. 1 the target temperature measured at the tube is almost stable after 30 minutes when the tube is cooled, whereas without tube cooling no steady state conditions are reached even after 300 minutes. This has to be taken into consideration when a high resolution XCT-measurement is performed. The measurements have to be taken after tube warm-up under conditions when the temperature is more or less constant. The decrease in maximum temperature also decreases instabilities of the specimen due to radiation.

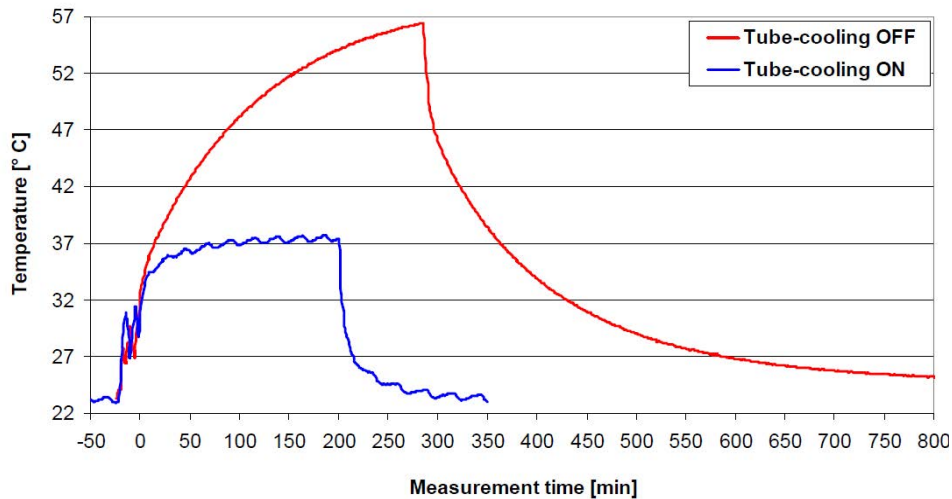


Figure 1. Temperature measured at the nanofocus-tube with and without tube cooling for the nanotom XCT-device.

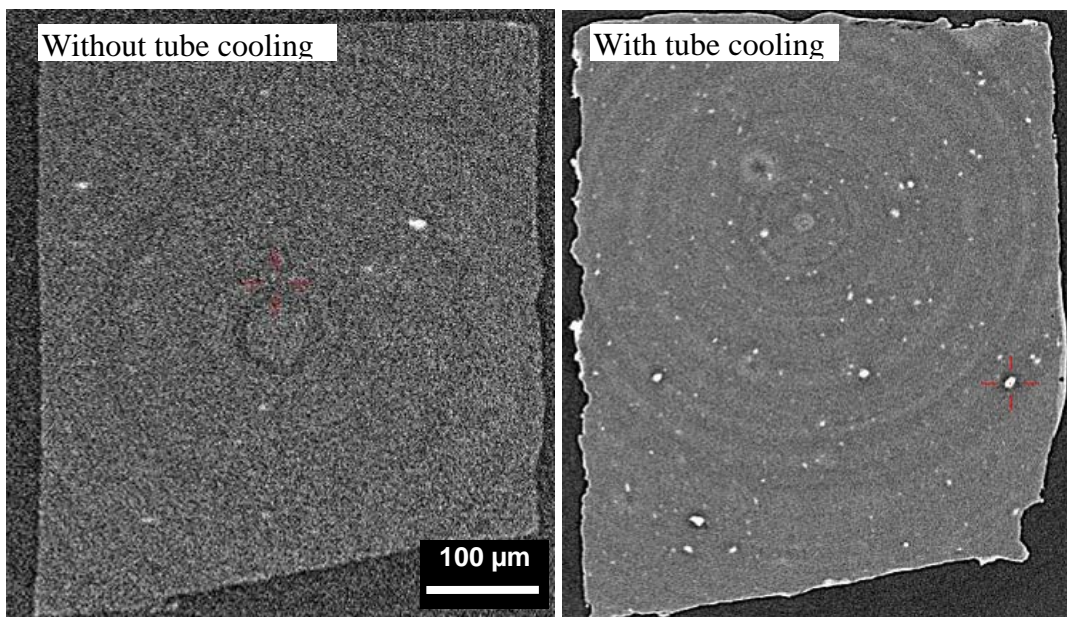


Figure 2. XCT-orthogonal cross-sectional pictures of polypropylene filled with talcum particles. The measurement on the left was performed without tube cooling and the measurement on the right was performed with cooling. The voxel size was $(0.7 \mu\text{m})^3$.

The improvement in image quality due to tube cooling and a small variation of measurement parameters is shown in Fig. 2 for a talcum filled polypropylene specimen at $0.7\ \mu\text{m}$ voxel size and a measurement time of nearly 7 hours. With tube cooling the noise is reduced and sharpness and detectability of details are increased significantly. Higher system stability leads also to a reduction of noise and the appearance of phase contrast. This could be explained by the fact that better stability of the location of the focal spot leads to higher coherence of the X-rays.

3.2 High resolution XCT results

This section shows the possibilities of high resolution cone beam XCT for non-destructive characterisation of materials. Figure 3 shows high resolution cone beam XCT results of wood measured with $1.5\ \mu\text{m}$ and $0.5\ \mu\text{m}$ voxel size. The change from early wood to late wood (year ring), a resin tube and the individual wood cells are clearly visible. On the edges of the sample some material deformations due to the chipping process are also visible. The picture on the right in Figure 3 shows walls of various wood cells, the thicknesses of the walls are about $2\ \mu\text{m}$. From these XCT-results it can be concluded that the XCT-resolution is $1\ \mu\text{m}$ or better.

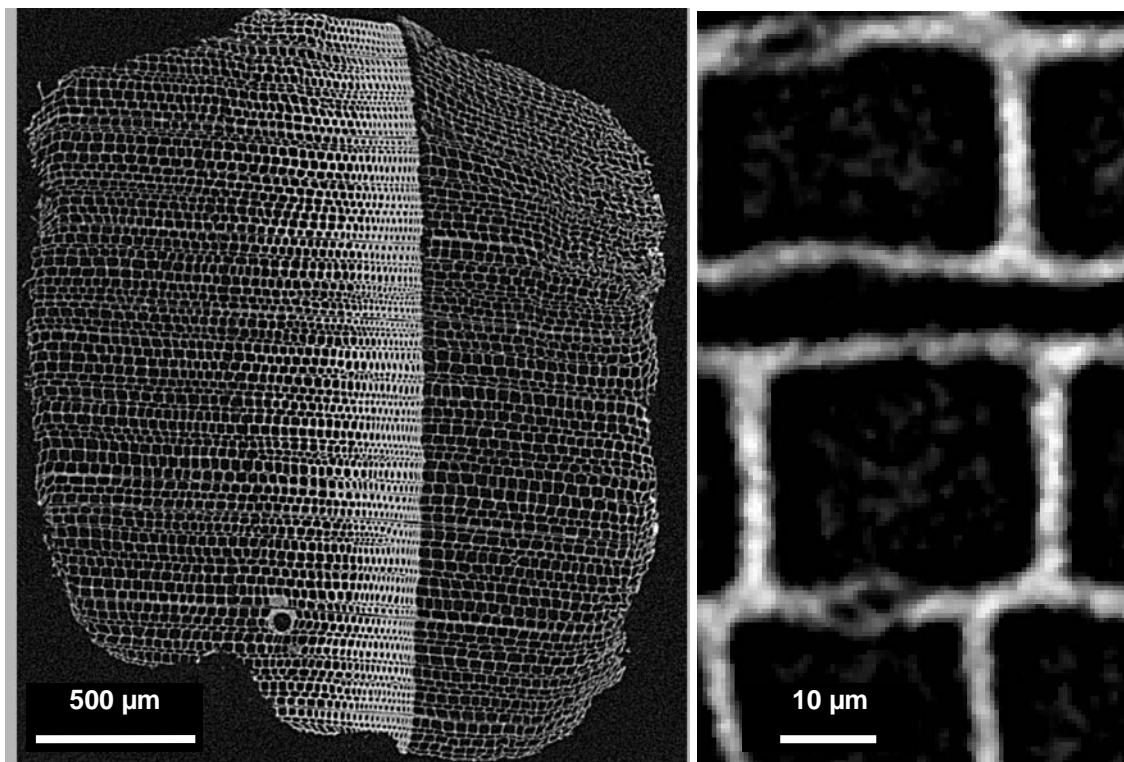


Figure 3. XCT- orthogonal cross-sectional pictures of pinewood. XCT-measurement was performed with $(1.5\ \mu\text{m})^3$ voxel size (left) and $(0.5\ \mu\text{m})^3$ (right). The picture on the right shows the walls of various wood cells with a thickness of about $2\ \mu\text{m}$.

Figure 4 shows a cross-sectional XCT-picture (left picture) and a 3D-representation (right picture) of the polyurethane foam filled with cellulose particles measured with a voxel size of $0.5\ \mu\text{m}$. The structures of this open cell foam and of the individual cellulose particles embedded in the polymer walls are clearly visible. Figure 4 also shows that the grey value at the polymer-air interface is much higher than within the polymer. This can be explained by a phase contrast effect caused by the small focal spot size and the high resolution of the XCT-measurement. A higher polymer density at the surface of the walls can be excluded [10]. It is known that phase contrast effects appear at these small focal spots, even for cone-beam XCT-systems with a polychromatic tube system. In Figure 5 orthogonal cross-

sectional XCT-pictures of gravity cast AlMg5Si7 are presented. Individual phases can be discriminated: high absorbing features $>5 \mu\text{m}$ in thickness are AlFeSi-phases and the lower absorbing features than from the Al-matrix can be identified as pores and coral like Mg_2Si -phases [11]. In all four different phases can be discriminated by high resolution XCT in this material.

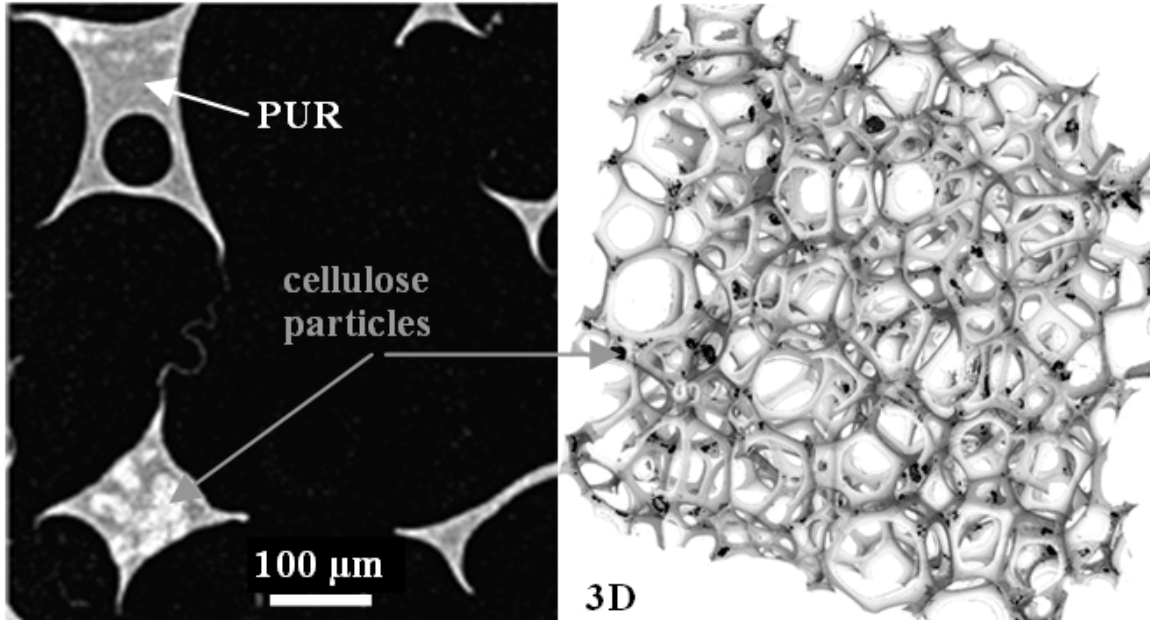


Figure 4. XCT-pictures of polyurethane (PUR) foam filled with cellulose particles (right pictures: cross-section and 3D-visualisation with the cellulose particles in black). XCT-measurement was performed with a voxel size of $(0.5 \mu\text{m})^3$.

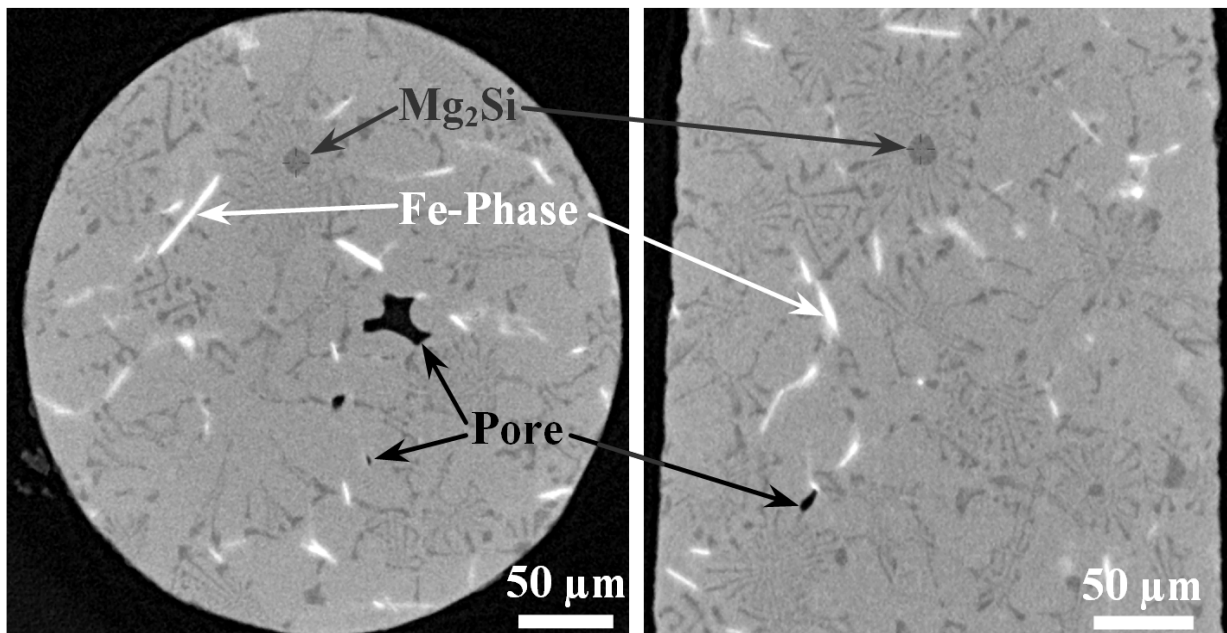


Figure 5. XCT-orthogonal cross-sectional pictures of AlMg5Si7. XCT-measurement was performed with a voxel size of $(0.5 \mu\text{m})^3$.

3.3 Phase contrast imaging

When X-ray attenuation coefficients at the interface between two different materials are too close, conventional absorption-based methods can fail to show a significant difference in

the resulting grey-values. In such cases phase-imaging methods can increase the contrast significantly and the edges can be enhanced. The influence of phase contrast on the resulting XCT-data and the detectability of details are shown in Figure 6. Here the object-detector distance ODD is increased from 189 to 486 mm, which results in an increase in the phase contrast.

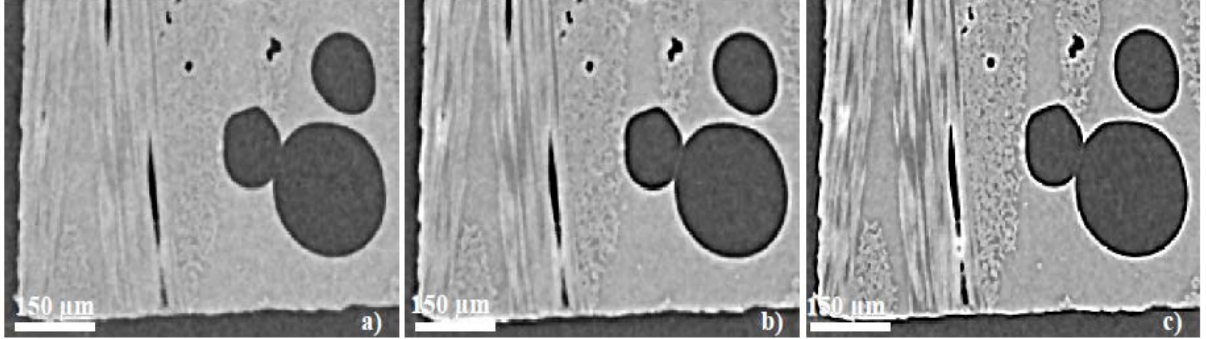


Figure 6. Cross-section of XCT-data of a carbon fibre reinforced polymer sample (CFRP) at different object-detector distances. The distance between the object and the detector is a) 189 mm, b) 283.5 mm and c) 486 mm. Voxel size was constant at $(2.75 \mu\text{m})^3$.

The increase in phase contrast with increasing distance between the object and the detector can be seen also in the grey value profiles along a certain pore. This is shown in the left graphic of Fig. 7. The corresponding absorption and phase contrast values for the various distances between the object and the detector are shown in the right graphic of Fig. 7.

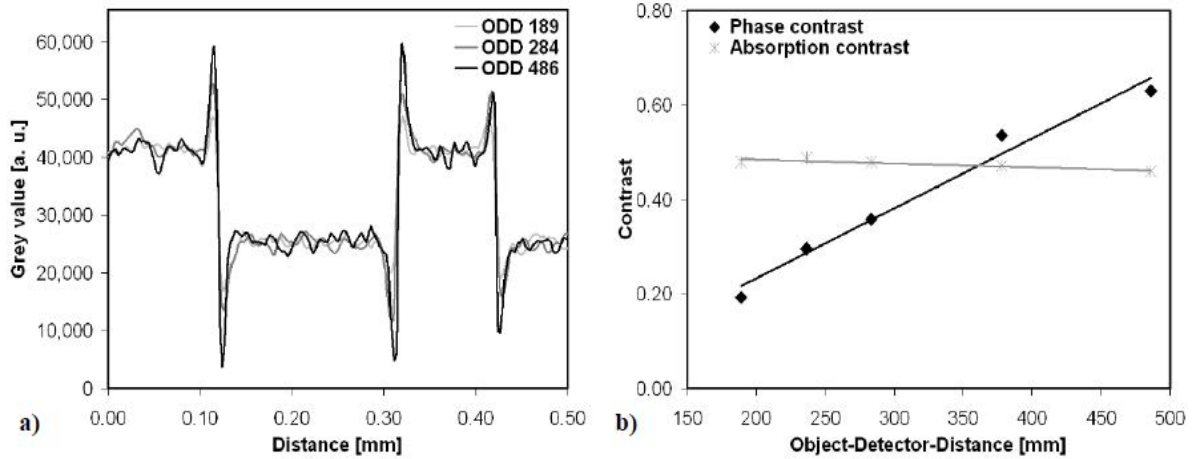


Figure 7. Grey-value profile along a pore from Fig.6 within the CFRP with different object-detector-distances (ODD) (a). Phase and absorption contrast versus object-detector-distance (b). Voxel size was $(2.75 \mu\text{m})^3$.

For calculating the absorption and phase contrast ($C_{Absorption}$ and C_{Phase}) the minimum grey-value intensity I_{min} close to the edge, the maximum grey value intensity I_{max} close to the edge, mean values for the grey-value intensities of the material I_{Mat} and the air within a pore I_{Air} were used in the following formulae.

$$C_{Absorption} = \frac{I_{Mat} - I_{Air}}{(I_{Mat} + I_{Air})/2}$$

$$C_{Phase} = \frac{I_{max} - I_{min} - (I_{Mat} - I_{Air})}{I_{max} + I_{min}}$$

The correction term $I_{Mat} - I_{Air}$ was included to obtain the sole phase contrast value without the absorption contrast. Fig. 7 shows an increase in phase contrast with increasing distance between the object and the detector, whereas the absorption does not change much. The influences of various measurement parameters on the phase contrast were studied and XCT measurements with different voxel sizes/resolutions and tube voltages were performed. Moreover, the appearance of XCT-phase contrast for the Al-alloy AlMg5Si7 was studied. The experimental results show that tomographic phase contrast behaves in a similar way to the CFRP sample shown above and to phase contrast in radiography:

- The phase contrast increases with increasing distance between the object and the detector (and with increasing distance between X-ray source and object). This is in accordance with phase contrast theory published by Wilkins et al [5] and Zhou et al [6].
- The phase contrast decreases with increasing tube voltage
- The phase contrast decreases with increasing focal spot size of the X-ray source
- The phase contrast is much lower for the higher absorbing Al-alloy AlMg5Si7, but a phase contrast effect is clearly recognisable. This is because the ratio of the refraction index and the absorption index δ/β in the X-ray region of the electromagnetic spectrum for the low density material CFRP (density at around 1.5 g/cm³) is much higher than that for the Al-sample with a density at around 2.7 g/cm³.

4. Conclusions and outlook

The results can be summarized in the following way:

- High resolution cone beam XCT is a powerful tool for non-destructive characterisation of materials. Voxel sizes below (0.5 μm)³ and resolutions around or slightly below 1 μm can be reached/achieved, when the stability of the XCT-system is good enough. For this purpose, and also for phase contrast tomography, appropriate tube cooling is a prerequisite. .
- The possibilities of high resolution cone beam XCT were demonstrated for various materials systems. XCT-results for polypropylene filled with talcum, for wood, for polyurethane foam filled with cellulose particles, for AlMg5Si7 and a carbon fibre reinforced polymer were presented.
- For high resolutions and for large distances between the object and the detector both phase and absorption contrasts are recognisable. The detectability of details is improved by the phase contrast.
- The phase contrast increases with increasing distance between the object and the detector, with decreasing tube voltage and with decreasing focal spot size. Phase contrast for the lower absorbing polymeric sample is much higher than for the Al-alloy.
- Further developments in terms of smaller focal spot sizes and high resolution XCT-systems will enhance the phase contrast effects and additional applications of phase contrast tomography in materials science can be expected.

5. Acknowledgements

The presented work was funded by the K-Project for non-destructive testing ZPT, grant number 820492 of the Austrian Research Promotion Agency (FFG). See <http://www.3dct.at> for further details. Thanks to Prof. Degischer and Dr. Requena of the Vienna University of Technology for fruitful discussions. We thank the companies Borealis, Lenzing, WOOD and FACC for delivering the samples.

References

- [1] J. Baruchel, J. Y. Buffiere, E. Maire, G. Peix (editors). X-ray tomography in material science. Paris: Hermes Science Publication; 2000.
- [2] J. Kastner (editor). Proceedings Industrielle Computertomografietagung. Aachen: Shaker Verlag; 2010.
- [3] P. Cloetens. Contribution to phase contrast imaging, reconstruction and tomography with hard synchrotron radiation, principles, implementation and applications. PhD thesis, Vrije Universiteit Brussel, Brussels, 1999.
- [4] D. Tisseur, J. M. Létang, J. Banchet. Phase contrast imaging in laboratory, Proceedings of DIR 2007 - International symposium on digital industrial radiology and computed tomography, Lyon, France, June 25-27, 2007.
- [5] S. W. Wilkins, T. E. Gureyev, D. Gao, A. Pogany, A. W. Stevenson. Phase-contrast imaging using polychromatic hard x-rays. *Nature* 1996; 384: 335-338.
- [6] S.-A. Zhou, A. Brahme. Development of phase-contrast X-ray imaging techniques and potential medical applications. *Physica Medica* 2008; 24: 129-148.
- [7] B. Zoofan, J.-Y. Kim, S. I. Rokhlina, G. S. Frankel. Application of phase contrast micro radiography in NDT. *Materials Evaluation* 2005; 1122-1127.
- [8] B. Zoofan, J.-Y. Kim, S. I. Rokhlina, G. S. Frankel. Phase contrast X-ray imaging for non-destructive evaluation of materials. *Journal of Applied Physics* 2006; 100: 014502-1 - 014502-7.
- [9] J. Kastner, B. Harrer, G. Requena, O. Brunke. A comparative study of high resolution cone beam X-ray tomography and synchrotron tomography applied to Fe- and Al-alloys. *NDT&E International* 2010; 43: 599-605.
- [10] J. Kastner, R. Kicking, D. Salaberger. High resolution X-ray computed tomography for 3D-microstructure characterisation of a cellulose particle filled polymer foam. *Journal of Cellular Plastics* 2011, accepted.
- [11] J. Kastner, B. Harrer, H.-P. Degischer. High resolution cone beam X-ray computed tomography for 3D-microstructure characterization of Al-alloys. *Materials Characterization* 2011; 62:99-107.